Fate of Two Mast Cell Tryptases in V3 Mastocytosis and Normal BALB/c Mice Undergoing Passive Systemic Anaphylaxis: Prolonged Retention of Exocytosed mMCP-6 in Connective Tissues, and Rapid Accumulation of Enzymatically Active mMCP-7 in the Blood

By Namit Ghildyal,* Daniel S. Friend,‡ Richard L. Stevens,* K. Frank Austen,* Chifu Huang,* John F. Penrose,* Andrej Šali,§ and Michael F. Gurish*

*From the Departments of *Medicine and ‡Pathology, Harvard Medical School; the *Division of Rheumatology and Immunology and the ‡Department of Pathology, Brigham and Women's Hospital, Boston, Massachusetts 02115; and §The Rockefeller University, New York 10021*

Summary

The mouse mast cell protease granule tryptases designated mMCP-6 and mMCP-7 are encoded by highly homologous genes that reside on chromosome 17. Because these proteases are released when mast cells are activated, we sought a basis for distinctive functions by examining their fates in mice undergoing passive systemic anaphylaxis. 10 min–1 h after antigen (Ag) was administered to immunoglobulin (Ig)E–sensitized mice, numerous protease/proteoglycan macromolecular complexes appeared in the extracellular matrix adjacent to most tongue and heart mast cells of normal BALB/c mice and most spleen and liver mast cells of V3 mastocytosis mice. These complexes could be intensively stained by anti-mMCP-6 Ig but not by anti-mMCP-7 Ig. Shortly after Ag challenge of V3 mastocytosis mice, large amounts of properly folded, enzymatically active mMCP-7 were detected in the plasma. This plasma-localized tryptase was ~150 kD in its multimeric state and ~32 kD in its monomeric state, possessed an NH_2 terminus identical to that of mature mMCP-7, and was not covalently bound to any protease inhibitor. Comparative protein modeling and electrostatic calculations disclosed that mMCP-6 contains a prominent Lys/Arg–rich domain on its surface, distant from the active site. The absence of this domain in mMCP-7 provides an explanation for its selective dissociation from the exocytosed macromolecular complex. The retention of exocytosed mMCP-6 in the extracellular matrix around activated tissue mast cells suggests a local action. In contrast, the rapid dissipation of mMCP-7 from granule cores and its inability to be inactivated by circulating protease inhibitors suggests that this tryptase cleaves proteins located at more distal sites.

A family of trypsin-like serine proteases is a major constituent of the secretory granules of certain populations of mast cells in mice (1–4) and humans (5–9). Two mouse tryptases (designated mouse mast cell protease [mMCP][1] 6 [2] and mMCP-7 [3]), whose genes reside on chromosome 17 (10, 11), have amino acid sequences that are 71% identical. The airway responsiveness of the C57BL/6 mouse to acetylcholine and 5-hydroxytryptamine is very low relative to other mouse strains (12), and linkage analysis (13) has implicated the region of chromosome 17 where the mMCP-6 and mMCP-7 genes reside as one of three candidate loci for the inheritance of intrinsic airway hyperresponsiveness. The observation that the C57BL/6 mouse cannot express mMCP-7 because its gene possesses a point mutation at its exon 2/intron 2 splice site (14) suggests a role of mMCP-7 in airway responsiveness. The additional finding that two low molecular weight inhibitors of tryptic enzymes block Ag-induced airway constriction and tissue inflammatory responses in *Ascaris suum*–sensitized sheep (15) supports the involvement of the tryptase family of mast cell proteases in the pathobiology of FcεRI-elicited responses in airways. Mast cell tryptases can induce airway smooth

[1] *Abbreviations used in this paper:* FPLC, fast protein liquid chromatography; mBMMC, mouse bone marrow–derived mast cell; mMCP, mouse mast cell protease; V3-MC, V3 mast cell.

 J. Exp. Med. © The Rockefeller University Press • 0022-1007/96/09/1061/13 $2.00
Volume 184 September 1996 1061–1073

muscle hyperresponsiveness in dogs (16), reverse airway smooth muscle relaxation induced by vasoactive intestinal peptide in the ferret (17), and induce proliferation of fibroblasts (18) and epithelial cells (19). Their physiologic substrates remain to be established; but in vitro studies have identified a number of susceptible substrates, including high molecular weight kininogen (20), vasoactive intestinal peptide (21), matrix pro-metalloproteinase-3 (22), pro-urokinase (23), fibronectin (24, 25), fibrinogen (26), and the complement protein C3 (27). That mMCP-6 and mMCP-7 have been implicated in airway reactivity prompted a more detailed consideration of the in vivo fate of these two tryptases after their exocytosis from tissue mast cells.

The secretory granules of mast cells possess a pH of ~5.5 (28). As a consequence, the 26–32-kD mMCPs that reside in secretory granules are positively charged and ionically bound to the various negatively charged serglycin proteoglycans in this intracellular compartment. Even at neutral pH, most mouse (1, 29), rat (30), and human (31, 32) granule proteases bind so strongly to serglycin proteoglycans that at least some of the macromolecular complexes exocytosed from mast cells activated by compound 48/80 or by cross-linking of their high affinity IgE receptors (FcεRI) remain intact outside of the cells for extended periods of time. Granule cores or remnants, reflecting protease/proteoglycan macromolecular complexes of undefined composition, have been observed outside of activated mast cells in tissues (33, 34) and in coculture with fibroblasts (35). The functional roles of the protease/proteoglycan macromolecular complexes remain to be determined, but serglycin proteoglycans have been reported to stabilize mast cell tryptases (31, 36) and alter the substrate specificities of mast cell tryptases and chymases (27, 37, 38).

Protein structure modeling and electrostatic calculations have been carried out for four chymases (mMCP-1, mMCP-2, mMCP-4, and mMCP-5) and the tryptase designated mMCP-7 (4, 39, 40). mMCP-4 and mMCP-5 were predicted to have two regions with net positive charges ranging from +6 to +10 at neutral pH located at opposite ends of each molecule and away from the substrate-binding cleft (39). mMCP-1, mMCP-2, and mMCP-7 are predicted to have only one of these regions. The putative glycosaminoglycan-binding regions in the four mast cell chymases are rich in Lys/Arg with at most one His residue. In contrast, the corresponding region in mMCP-7 has five His residues. Thus, in distinction to the chymases, the strong positive potential on one face of mMCP-7 is diminished at neutral pH where the His residues do not have a positive charge. Site-directed mutagenesis of recombinant pro-mMCP-7 showed that the mutation of His^{8}, His^{68}, or His^{70} into a Glu residue in the identified positively charged region prevents its binding to heparin at pH 5.5 (40). These in vitro observations raised the possibility that mMCP-7 might selectively dissociate from its proteoglycan/protease macromolecular complexes in vivo after exocytosis into a neutral pH environment such as the extracellular milieu. To test this hypothesis, we examined the fate of two homologous but distinct tryptases exocytosed in vivo from FcεRI-activated mouse mast cells.

Materials and Methods

FcεRI-mediated Activation of Mast Cells in V3 Mastocytosis Mice and in Normal BALB/c Mice. To create a V3 mastocytosis mouse, ~10^6 cultured V3 mast cells (V3-MC), maintained in enriched RPMI-1640 medium as described previously (41), were injected intravenously into the tail vein of a 6-wk-old BALB/c mouse (The Jackson Laboratory, Bar Harbor, ME). V3 mastocytosis mice were used 2–4 wk after the adoptive transfer of V3-MC. Anti-TNP IgE was diluted in HBSS to a final concentration of 1 mg/ml, and V3 mastocytosis and normal BALB/c mice were each sensitized with 200 μg IgE i.p. Alternatively, each mouse was sensitized with 100 μl i.p. of an ascites fluid preparation of IgE. Ascites IgE was titered for activity by passively sensitizing mice and monitoring plasma histamine levels 15 min after administration of Ag (TNP-BSA). The dose of ascites used in the in vivo experiments mediated a level of histamine release comparable with that obtained with 200 μg of purified IgE. 24 h after passive sensitization, TNP-BSA in ~300 μl of HBSS was injected intraperitoneally into each mouse. Normal sensitized mice generally received 1,000 μg Ag. Depending on the extent of the disease, the amount of Ag given to an IgE-sensitized V3 mastocytosis mouse varied from 10 to 1,000 μg. The IgE and Ag dosages used in each experiment produced obvious symptoms of mast cell activation (e.g., labored breathing and decreased movement) but no mortality. 10 min–24 h after Ag administration, 100–500 μl of blood was obtained from the retroorbital plexus with a Pasteur pipette pretreated with an anticoagulant. Each plasma sample contained either 25 U of heparin glycosaminoglycan (Elkins-Sinn, Cherry Hill, NC) or 10 mM EDTA. Samples were centrifuged for 3–5 min at ~10,000 *g* at 4°C.

Preparation of Anti-mMCP-6 Ig. The preparation and specificity of anti-mMCP-6 Ig has not been described, but this rabbit anti–peptide Ab was used in the initial characterization of the V3 mastocytosis mouse (41). Although the overall amino acid sequences of mMCP-6 and mMCP-7 are 71% identical (2–4), areas of greater dissimilarity are present in the tryptases. Since a mMCP-7–specific Ab was previously obtained in rabbits with a synthetic 19-mer peptide (designated peptide 7) that corresponds to residues 160–178 (42), an Ab was prepared against a synthetic peptide (designated peptide 6) that corresponds to the analogous region in mMCP-6 (Fig. 1 *A*). As assessed by the Protein Identification Resource database of the National Biomedical Foundation (Bethesda, MD), peptide 6 (Arg-Lys-Try-His-Thr-Gly-Leu-Try-Thr-Gly-Asp-Asp-Phe-Pro-Ile-Val-His-Asp-Gly) is not present in any other mouse protein. This peptide was synthesized by Bioserv Labs (San Jose, CA) coupled to an octavalent Lys resin. A New Zealand White rabbit was injected intramuscularly with an emulsion consisting of 0.5 ml of the coupled peptide (~500 μg) mixed with an equal volume of TiterMax synthetic adjuvant (CyRx Corp., Norcross, GA). The immunized rabbit received booster injections intramuscularly 4 and 12 wk later, and its serum was then collected at biweekly intervals over a number of months. To purify anti-mMCP-6 Ig, a ~20-μg portion of peptide 6 was coupled at 4°C to 4 ml of Affi-Gel 10 (Bio-Rad Laboratories, Richmond, CA) in 0.1 M sodium bicarbonate, pH 8.5. An affinity column was prepared by equilibrating the resin with 16 mM boric acid/0.15 M NaCl, pH 8.0. A 10-ml sample of antiserum was applied, and the bound Ab was eluted with 10 ml of

100 mM glycine-HCl, pH 2.5, followed by 10 ml of 0.1 M triethylamine, pH 11.0, into a neutralizing buffer of 2 M Tris-HCl, pH 8.0. The collected fractions were pooled, dialyzed against PBS, and stored at −20°C. As assessed by SDS-PAGE, the resulting affinity-purified Ab consisted primarily of IgG. This rabbit Ab reacted with peptide 6 in an ELISA at an >10,000-fold dilution. The concentration of affinity-purified anti-mMCP-6 Ig was estimated by optical density. Relative to mature mast cells (1), mouse bone marrow–derived mast cells (mBMMC) contain very low amounts of serine protease (24). Nevertheless, SDS-PAGE/immunoblot analysis revealed that affinity-purified anti-mMCP-6 Ig recognized an ~32-kD protein in lysates of 1–2 × 10^6 BALB/c mBMMC (Fig. 1 *B*) developed with IL-3–enriched conditioned medium (43). The 32-kD protein was not recognized by preimmune serum (data not shown), and reactivity could be blocked by preincubation of the antiserum with peptide 6 but not with the peptide that corresponds to the homologous region in mMCP-7 (Fig. 1 *B*). Using the same cell equivalents, the sensitivity of the SDS-PAGE/immunoblot assay with anti-mMCP-6 Ig was found to be comparable with that obtained with anti-mMCP-7 Ig (42).

Immunohistochemical and Histochemical Analyses of FcεRI-activated Tissue Mast Cells of Normal BALB/c Mice and V3 Mastocytosis Mice. For immunoalkaline phosphatase staining (44), isolated tissues were fixed for 4 h at room temperature in 4% paraformaldehyde and 0.1 M sodium phosphate, pH 7.6 (45). Preparations were washed twice with PBS containing 2% DMSO and then were suspended in 50 mM NH_4Cl overnight at 4°C. The specimens were dehydrated and embedded in accordance with the JB-4 embedding kit instructions from Polysciences Inc. (Warrington, PA). After 1–2 d of hardening, 1.5-μm-thick sections of fixed and embedded tissue were cut on a Reichert-Jung Supracut microtome (Leica, Deerfield, IL) with glass knives and picked up on glass slides. The slides were incubated sequentially for 15 min at 37°C in 2 mM $CaCl_2$ containing 0.025% pancreatic trypsin, for 15 min at room temperature in PBS containing 0.05% Tween-20 and 0.1% BSA, for 30 min at 37°C in PBS containing 0.05% Tween-20 and 4% normal goat serum, and overnight at 4°C in 4% normal goat serum containing affinity-purified rabbit anti-mMCP-6 Ig or anti-mMCP-7 Ig (42). The samples were washed and incubated for 40 min at room temperature in buffer containing biotin-labeled goat anti–rabbit IgG. Each was washed twice in 0.1% BSA and 0.05% Tween-20 in PBS, incubated for 40 min at room temperature in Vectastain ABC-AP reagent (Vector Laboratories, Inc., Burlingame, CA), and then incubated for 15 min in the dark at room temperature in an alkaline phosphatase substrate solution. Controls consisted of sections of tissue from normal mice and V3 mastocytosis mice treated with nonimmune IgG (Endogen, Inc., Boston, MA) or without primary Ab. Tissue sections were counterstained with Gill's hematoxylin in 20% ethylene glycol, and then coverslips with ImmuMount (Shandon, Inc., Pittsburgh, PA) were applied.

For histological examination, serial 1.5-μm-thick glycol-methacrylate-embedded sections of various tissues from normal BALB/c mice and from V3 mastocytosis mice were placed on coverslips or slides, air dried, and stained for 20 s in a 5% ethanolic solution of methylene blue (46). Alternatively, sections were incubated sequentially with double-strength hematoxylin for 2 min, 1% aqueous eosin Y for 15 min, azure II for 1 min, and ethylene glycol monomethyl ether for 5 s.

SDS-PAGE/Immunoblot Analysis of Plasma for Mast Cell Tryptases and Characterization of Plasma-localized mMCP-7. Samples of plasma (~5 μl) or BALB/c mBMMC lysates (~10^6 cell equivalents) were diluted 1:5 vol/vol in SDS-PAGE buffer (1% SDS, 5% 2-ME, 0.1% bromophenol blue, and 500 mM Tris-HCl, pH 6.8) and boiled for 5 min before being loaded onto 12% polyacrylamide gels. After SDS-PAGE, the resolved proteins were transferred in 20 mM Tris-HCl, 150 mM glycine, pH 8.3 buffer containing 20% methanol for 2–4 h at 200 mA to an Immobilon-P membrane (Millipore Corp., Bedford, MA) using an immunoblotting apparatus (Bio-Rad Laboratories). The resulting blots were preincubated in blocking solution (Bio-Rad Laboratories) for at least 4 h at 4°C. Anti-mMCP-6 Ig or anti-mMCP-7 Ig was then added, and each blot was incubated overnight at room temperature in a sealed plastic bag. After three 30-min washes, the secondary Ab (diluted in blocking solution containing 1% normal goat serum [The Jackson Laboratory]) was added, and the blot was again incubated overnight at room temperature. Each immunoblot was then washed and developed with a chemiluminescence kit from Dupont/New England Nuclear (Boston, MA).

Heparin-Sepharose chromatography (40) was used to determine whether or not plasma-localized mMCP-7 was properly folded and associated with another protein. 200 μl of pooled plasma from FcεRI-activated V3 mastocytosis mice were applied to a 1-ml column of heparin-Sepharose CL-6B (Pharmacia, Piscataway, NJ) equilibrated in 100 mM NaCl/10 mM sodium phosphate, pH 5.0 buffer. The bound proteins were eluted with a step gradient in which the NaCl concentration of the buffer was sequentially increased to 200 mM, then to 300 mM, and finally to 400 mM. Four 0.5-ml fractions were collected for each step; 0.1-ml samples of each fraction were applied to an Immobilon-P membrane and analyzed for the presence of immunoreactive mMCP-7, as described above. The protein content of each fraction was also estimated with a protein assay kit from Bio-Rad Laboratories.

The major form of mMCP-7 in the plasma samples was isolated by fast protein liquid chromatography (FPLC). 100 μl of pooled plasma from FcεRI-activated V3 mastocytosis mice were loaded on a Superose 12 HR 10/30 gel filtration column (Pharmacia) that had been equilibrated in 150 mM NaCl/10 mM EDTA/10 mM sodium phosphate, pH 7.35. The column was eluted at a flow rate of ~0.25 ml/min, and 0.25–0.5-ml fractions were collected and analyzed for the presence of immunoreactive mMCP-7. To obtain its NH_2-terminal sequence, the fraction containing the most immunoreactive mMCP-7 was subjected to preparative SDS-PAGE. Resolved proteins were transferred to an Immobilon-P membrane. One lane of the protein blot was analyzed for the presence of immunoreactive mMCP-7. The other lane was briefly stained with 0.5% Ponceau S (Sigma Chemical Co., St. Louis, MO). The 32-kD protein in this lane, which was recognized by anti-mMCP-7 Ig in the replicate blot, was excised, placed in the reaction cartridge of a gas-phase sequencer (model 470A; Applied Biosystems, Foster City, CA), and subjected to automated Edman degradation at the Harvard Microchemistry Facility.

The spectrophotometric method of Svendsen et al. (47) was used to determine whether or not plasma-localized mMCP-7 is enzymatically active. A 1–20-μl sample of a plasma or column fraction was placed in 1 ml of a pH 7.6 buffer containing 25 mM sodium phosphate, 1 mM EDTA, and 50 μg of tosyl-Gly-Pro-Lys-*p*-nitroanilide, benzoyl-Ile-Glu-Gly-Arg-*p*-nitroanilide, acetyl-Ile-Glu-Ala-Arg-*p*-nitroanilide, or D-Ile-Phe-Lys-*p*-nitroanilide. The change in optical density at 405 nm was then measured at room temperature. These synthetic peptide substrates were selected because pancreatic trypsin readily cleaves all four, whereas

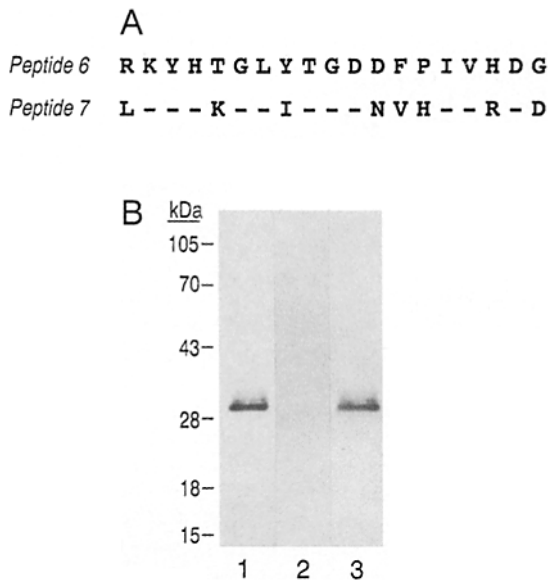

Figure 1. SDS-PAGE/immunoblot analysis of lysates of ~10^6 cell equivalents of BALB/c mBMMC using anti-mMCP-6 Ig. (*A*) The amino acid sequences of peptides 6 and 7 that correspond to residues 160–178 in mMCP-6 (2) and mMCP-7 (3), respectively. (*Dash*) An identical amino acid. (*B*) SDS-PAGE/immunoblot analysis of lysates of mBMMC probed with anti-mMCP-6 Ig in the absence of any synthetic peptide (lane *1*), or in the presence of peptide 6 (lane *2*) or peptide 7 (lane *3*). Molecular weight markers are indicated on the left.

recombinant mature mMCP-7 selectively degrades tosyl-Gly-Pro-Lys-*p*-nitroanilide (Huang, C., R. Matsumoto, and R.L. Stevens, unpublished findings). Each assay was standardized with recombinant mMCP-7.

Comparative Protein Modeling and Electrostatic Calculations for mMCP-6 and mMCP-7. As described previously for mMCP-1, mMCP-2, mMCP-4, mMCP-5, and mMCP-7 (39, 40), a three-dimensional model of mMCP-6 was built by MODELLER-3 (MODELLER is available by anonymous FTP from guitar.rockefeller.edu and also as part of QUANTA and INSIGHTII [MSI, San Diego, CA; e-mail blp@msi.com].) (48, 49) with the crystallographic structure of bovine pancreatic trypsin (Bookhaven Protein Data Bank code 2PTN) (50) used as the template. The model of mMCP-6 passes all the stereochemistry checks implemented in the program PROCHECK-3 (51). The electrostatic potentials of mMCP-6 and mMCP-7 at pH 7.0 were calculated with the GRASP program (52), with standard charges from the CHARMM-22 force field (53). Each Lys and Arg residue was assigned a positive charge, each Glu and Asp residue was assigned a negative charge, and each His residue was assigned a neutral charge.

Results

Histochemical and Immunohistochemical Analyses of Tissue Mast Cells After Passive Systemic Anaphylaxis. As assessed histochemically and immunohistochemically, mMCP-6 and mMCP-7 are both present in the methylene blue–staining granules of the mast cells that reside in normal, striated muscle-containing tissues such as the tongue (Fig. 2) and heart (Fig. 3) of the BALB/c mouse. Both Abs stained non-activated mast cells with approximate equal intensity. 10–15 min after Ag was administered to IgE-sensitized BALB/c mice, numerous methylene blue–staining granule cores were found outside of most mast cells in these two tissues. The granule cores were more frequently and more intensely stained by anti-mMCP-6 Ig than by anti-mMCP-7 Ig. Approximately 1 h after Ag administration, the extracellular matrix adjacent to most activated tongue and heart mast cells still contained large numbers of granule cores that stained with methylene blue and anti-mMCP-6 Ig but not with anti-mMCP-7 Ig.

To investigate the differential fate of these granule constituents in more depth after their release into the extracellular matrix, V3 mastocytosis mice were subjected to passive systemic anaphylaxis. Spleen and liver were analyzed because of their large content of mMCP-6$^+$/mMCP-7$^+$ mast cells (41). When IgE-sensitized V3 mastocytosis mice were given buffer alone intraperitoneally (n = 5), no methylene blue$^+$/mMCP-6$^+$/mMCP-7$^+$ granule cores were found in the extracellular matrix of the liver (Fig. 4) or spleen (data not shown). The granule cores present in the extracellular matrix 10 min after systemic Ag challenge of replicate IgE-sensitized mice were strongly stained by methylene blue and by anti-mMCP-6 Ig (n = 8). Even though the nonexocytosed granules in these FcεRI-activated mast cells were readily stained by anti-mMCP-7 Ig, their exocytosed granule cores were only weakly stained by this Ab. 1 h after Ag challenge, large numbers of granule cores remained in the extracellular matrix that were stained with methylene blue and anti-mMCP-6 Ig but not anti-mMCP-7 Ig (Fig. 4).

SDS-PAGE/Immunoblot Analysis of Plasma for the Two Mast Cell Tryptases and Characterization of Plasma-localized mMCP-7 by Size, Function, and NH_2-terminal Amino Acid Sequence. SDS-PAGE/immunoblot analysis was used to determine whether or not any exocytosed mMCP-7 could make its way into the plasma of FcεRI-activated V3 mastocytosis mice. No immunoreactive mMCP-7 could be detected in the plasma of normal BALB/c mice that had been induced to undergo passive systemic anaphylaxis (Fig. 5). However, a 32-kD protein was recognized by SDS-PAGE/immunoblot analysis with anti-mMCP-7 Ig in the plasma of IgE-sensitized V3 mastocytosis mice 10–20 min after Ag administration (n = 5) (Fig. 5). Although this immunoreactive protein was still present in abundance 1 h after systemic Ag administration, no immunoreactive mMCP-7 was detected in the plasma after 4 h. In four of the five experiments, the level of immunoreactive mMCP-6 in the plasma samples was below detection at all time points (Fig. 5). However, in a single experiment, a very small amount of mMCP-6 was detected in plasma at the 1- and 4-h time points (data not shown).

The immunoreactive protein present in the plasma 20 min after the administration of Ag to IgE-sensitized mice bound to a heparin-Sepharose column that had been equilibrated in 100 mM NaCl/10 mM sodium phosphate, pH 5.5. Because it dissociated from the affinity column when the NaCl concentration of the buffer was raised to ~300 mM (data not shown), analogous to properly folded re-

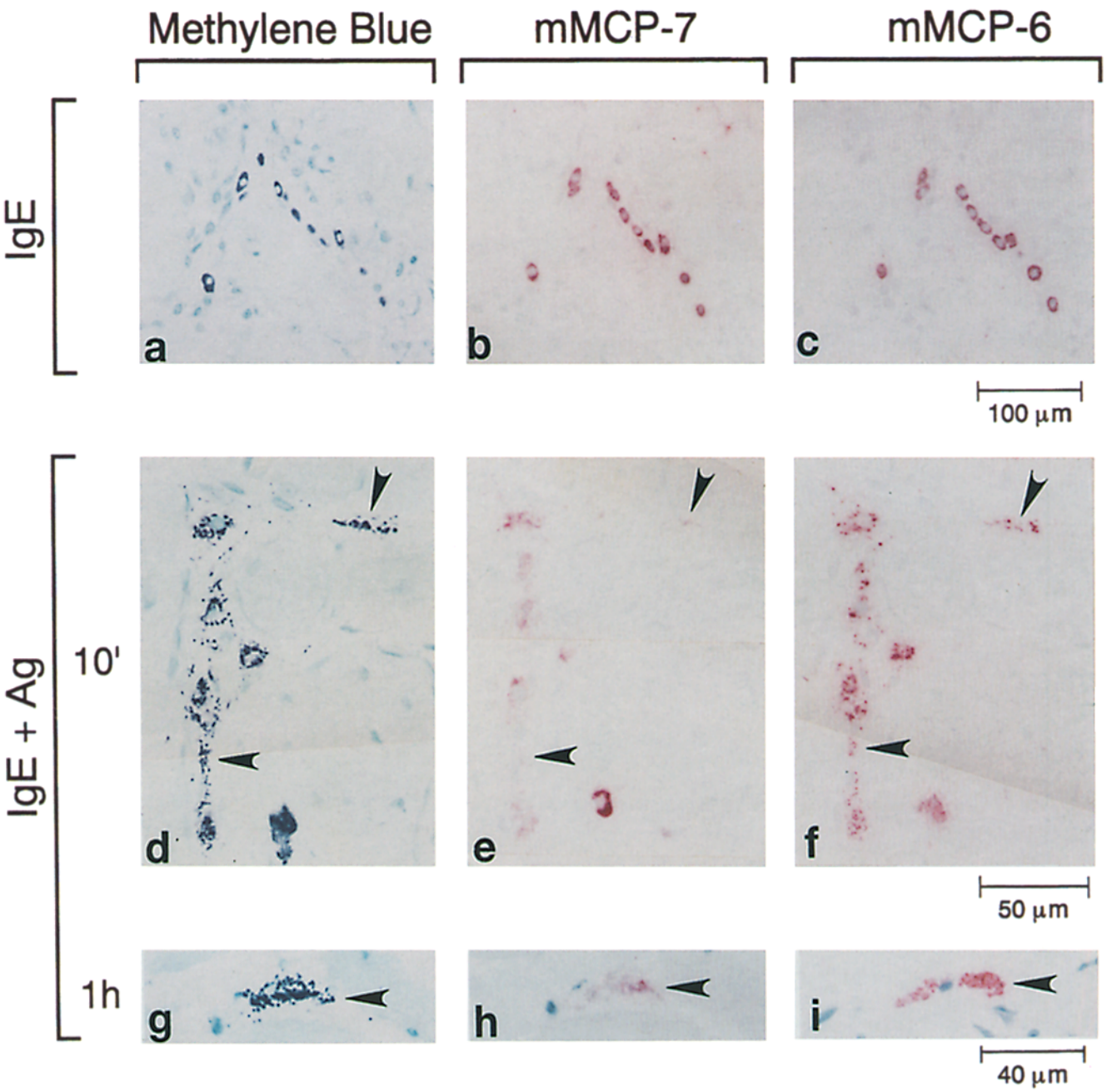

Figure 2. Immunohistochemical and histochemical analyses of the exocytosed tryptase/proteoglycan complexes remaining in the tongue around FcεRI-activated mast cells. Serial sections of tongue tissue, prepared from IgE-sensitized normal BALB/c mice (*a–c*) or from IgE-sensitized normal BALB/c mice 10 min (*d–f*) and 1 h (*g–i*) after Ag challenge, were stained with methylene blue (*a*, *d*, and *g*), anti-mMCP-7 Ig (*b*, *e*, and *h*), or anti-mMCP-6 Ig (*c*, *f*, and *i*). (*Arrows*) Exocytosed granule cores in the extracellular matrix.

combinant pro and mature mMCP-7 (40), plasma-localized mMCP-7 appeared to be in its native state and not associated with another plasma protein. Furthermore, plasma samples obtained within 30 min after Ag challenge of IgE-sensitized V3 mastocytosis mice readily cleaved tosyl-Gly-Pro-Lys-*p*-nitroanilide but not benzoyl-Ile-Glu-Gly-Arg-*p*-nitroanilide, acetyl-Ile-Glu-Ala-Arg-*p*-nitroanilide, or D-Ile-Phe-Lys-*p*-nitroanilide ($n = 3$). Compared with recombinant mMCP-7, the amount of enzymatically active mMCP-7 in the different plasma samples ranged from 50 to 500 μg/ml. No tryptase activity was detected in the plasma of IgE-sensitized V3 mastocytosis mice that were not challenged with Ag.

Although SDS-PAGE immunoblot analysis indicated that the major form of mMCP-7 in the plasma was ~32 kD, this immunoreactive protein and the tryptase activity cochromatographed on the FPLC column as a broad peak with an apparent average molecular mass of ~150 kD,

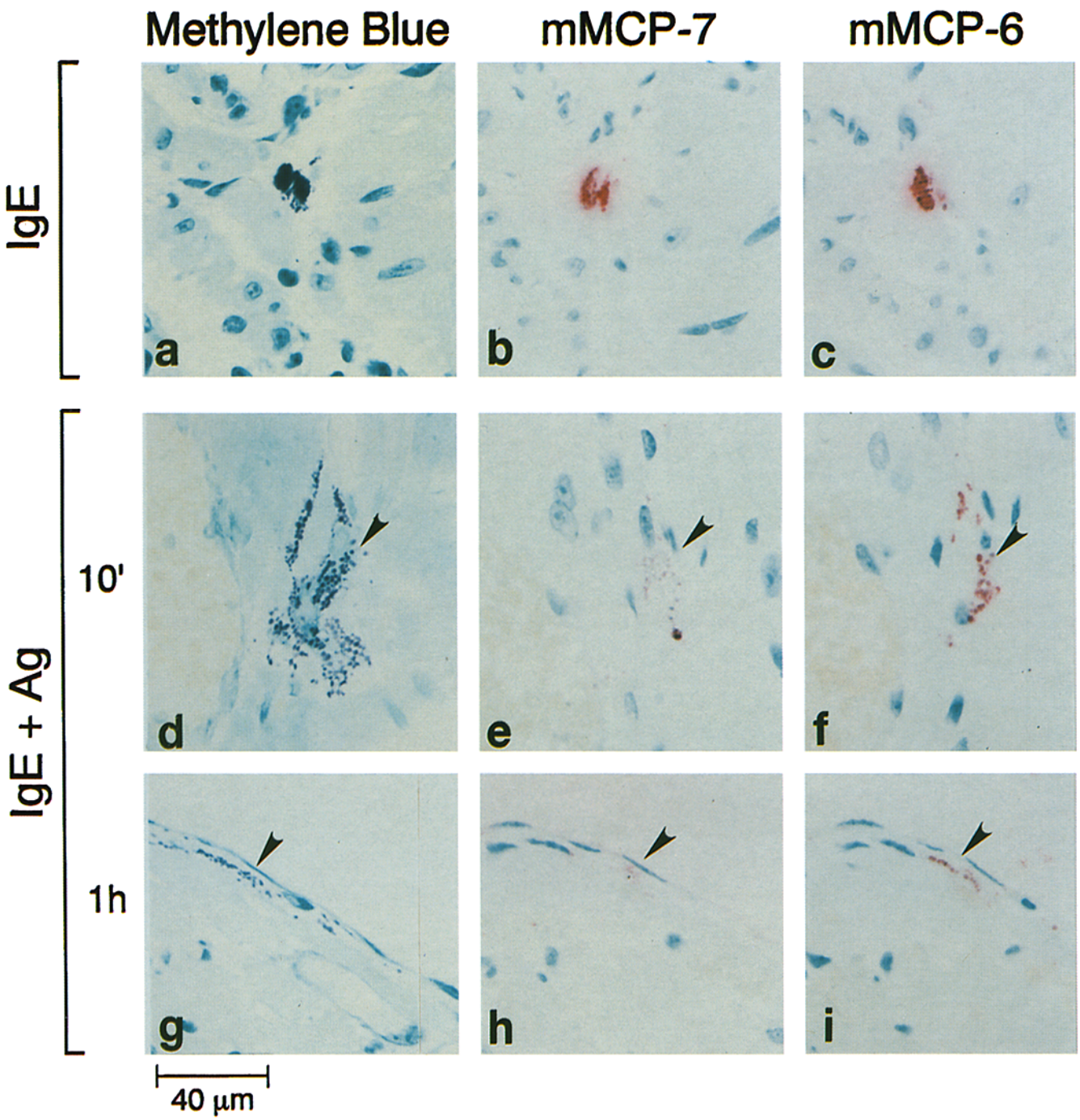

Figure 3. Immunohistochemical and histochemical analyses of the exocytosed tryptase/proteoglycan complexes remaining in the heart around FcεRI-activated mast cells. Serial sections of heart tissue, prepared from IgE-sensitized normal BALB/c mice (*a–c*) or from IgE-sensitized normal BALB/c mice 10 min (*d–f*) and 1 h (*g–i*) after Ag challenge, were stained with methylene blue (*a*, *d*, and *g*), anti-mMCP-7 Ig (*b*, *e*, and *h*), or anti-mMCP-6 Ig (*c*, *f*, and *i*). (*Arrows*) Exocytosed granule cores in the extracellular matrix.

whether heparin or EDTA (Fig. 6) was employed as the anticoagulant. In one experiment, the serum was pooled from three mice and the FPLC fraction containing the peak level of the immunoreactive protein was concentrated and subjected to preparative SDS-PAGE. After transfer to an Immobilon-P membrane and NH_2-terminal amino acid analysis of the immunoreactive 32-kD protein, a single prominent sequence of Ile-Val-Gly-Gly-Gln-Glu-Ala-His-Gly-Asn-Lys-Trp-Pro-Trp was obtained. This sequence is identical to the NH_2-terminal amino acid sequence of mature mMCP-7 deduced from its cDNA and gene (3).

FcεRI-dependent Activation of BALB/c mBMMC and Evaluation of the Exocytosed Macromolecular Complexes for mMCP-6. Blots previously used for evaluating the extracellular re-

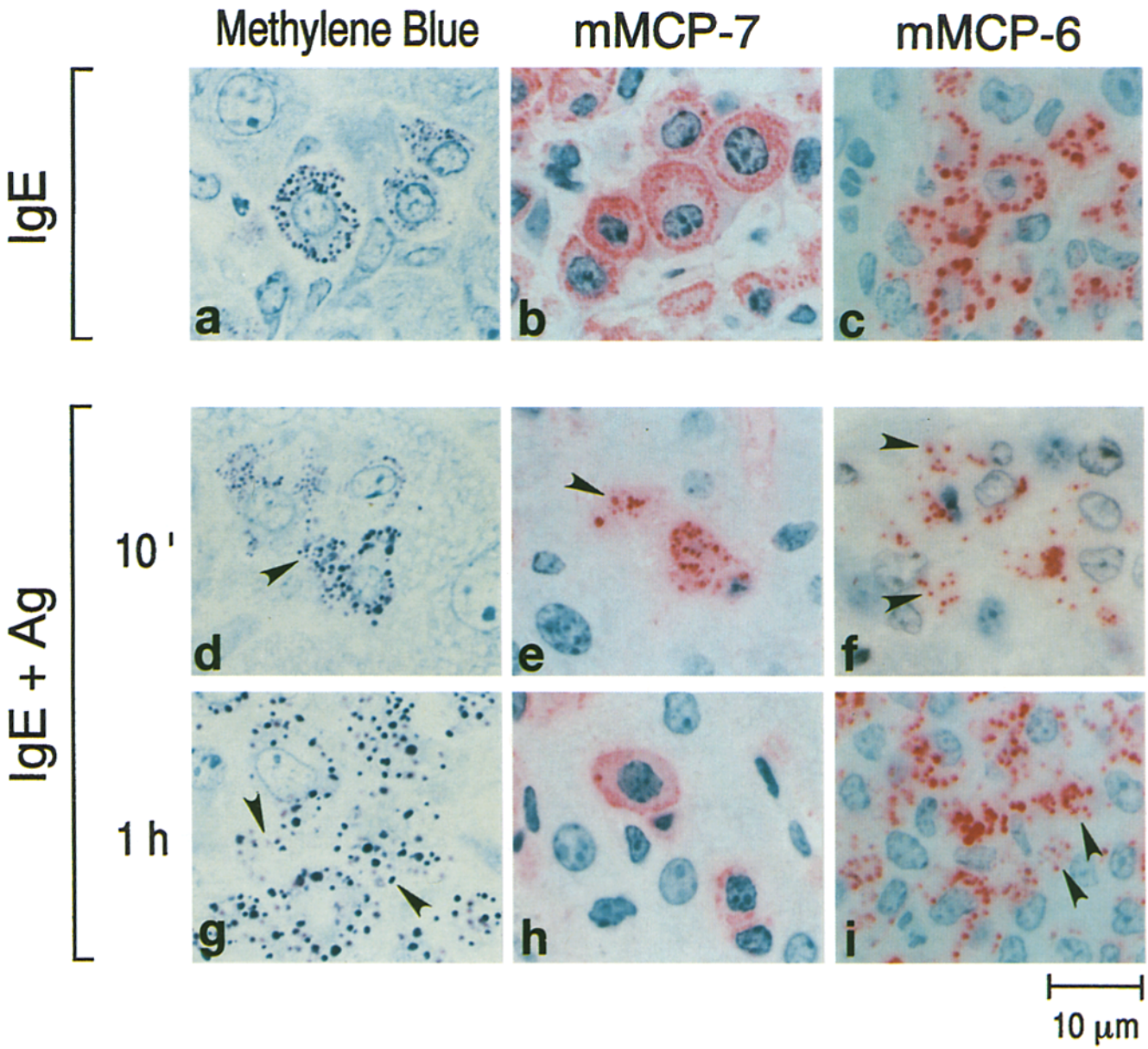

Figure 4. Immunohistochemical and histochemical analyses of the exocytosed tryptase/proteoglycan complexes remaining in the liver around FcεRI-activated V3-MC. Serial sections of liver tissue, prepared from IgE-sensitized V3 mastocytosis mice (*a–c*) or from IgE-sensitized V3 mastocytosis mice 10 min (*d–f*) and 1 h (*g–i*) after Ag challenge, were stained with methylene blue (*a*, *d*, and *g*), anti-mMCP-7 Ig (*b*, *e*, and *h*), or anti-mMCP-6 Ig (*c*, *f*, and *i*). (*Arrows*) Exocytosed granule cores in the extracellular matrix.

tention of mMCP-5 and mMCP-7 in the granule core complexes (40) are now reported for the concurrent findings with anti-mMCP-6 Ig. In these in vitro studies, BALB/c mBMMC were sensitized with anti-TNP IgE, washed, and challenged with TNP-BSA. The FcεRI-activated mBMMC were sedimented and samples of the resulting supernatants were applied to a column of Sepharose CL-2B that had been equilibrated with Tris-buffered saline, pH 7.2. Protein blots containing samples of each column fraction were analyzed not only as described (40) but also with anti-mMCP-6 Ig. In each of four experiments, the majority of immunoreactive mMCP-6 filtered in the column's excluded volume (data not shown).

Comparative Protein Modeling and Electrostatic Calculations for mMCP-6 and mMCP-7. The backbone structure of the mMCP-6 model is virtually indistinguishable from that of the mMCP-7 model. The three-dimensional model of mMCP-6 suggests that, as with mMCP-7, there is a trypsinlike fold consisting of two domains with the active site located in the cleft at their interface. A region was identified on the surface of mMCP-6 away from the active site that likely possesses a very strong positive potential at pH 7.0 (Fig. 7 *A*). This region contains seven Lys residues (Lys^{11}, Lys^{146}, Lys^{149}, Lys^{161}, Lys^{201}, Lys^{203}, and Lys^{223}) and three Arg residues (Arg^{160}, Arg^{186}, and Arg^{187}). Whereas mMCP-7 has a His-rich region that is positively charged at

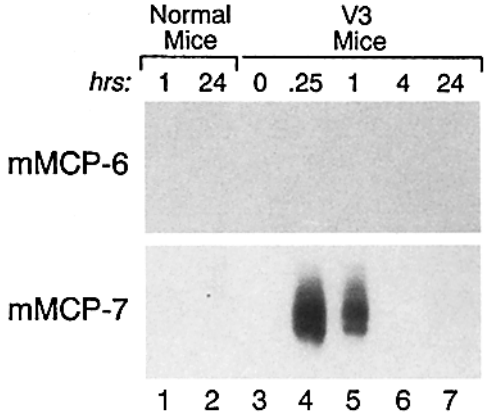

Figure 5. Time course of appearance and disappearance of immunoreactive mast cell tryptases in the circulation of FcεRI-activated mice. In the depicted representative experiment, plasma samples were collected from IgE-sensitized normal BALB/c mice (lanes *1* and *2*) and V3 mastocytosis mice (lanes *3*–*7*) at various time intervals after Ag administration. The samples were subjected to SDS-PAGE/immunoblot analysis, probing with anti-mMCP-6 Ig or anti-mMCP-7 Ig.

the granule pH of 5.5 (40), it lacks a Lys/Arg–rich region on any of its faces (Fig. 7 *B*).

Discussion

We now report on the preferential retention of mMCP-6 in tissues and the preferential release of mMCP-7 into the plasma from FcεRI-activated mast cells in vivo. Immunoreactive mMCP-6 and mMCP-7 are each present in the granules of the mast cells that reside in the tongue and heart of normal BALB/c mice (Figs. 2 and 3) and in the granules of the transformed mast cells that develop in the liver and spleen of V3 mastocytosis mice (Fig. 4). 10–15 min after Ag was administered to IgE-sensitized normal BALB/c mice or V3 mastocytosis mice, numerous granule cores composed of protease/proteoglycan macromolecular complexes were detected in the extracellular matrix adjacent to activated mast cells. 1 h after passive systemic anaphylaxis, the extracellular matrix adjacent to activated mast cells in the tongue and heart of normal mice or in the liver and spleen of V3 mastocytosis mice still contained large numbers of methylene blue–staining granule cores that also contained immunoreactive mMCP-6. In contrast, extracellular immunoreactive mMCP-7 was depleted by 10 min.

BALB/c mBMMC express mMCP-5 (54), mMCP-6 (2), and mMCP-7 (3). When supernatants from FcεRI-activated mBMMC were chromatographed on a Sepharose CL-2B column, the majority of immunoreactive mMCP-5 filtered in the column's excluded volume as a large macromolecular complex with serglycin proteoglycans, whereas nearly all immunoreactive mMCP-7 filtered in the column's included volume (40). Analysis of replicate protein blots from these same experiments with anti-mMCP-6 Ig revealed that in all experiments, the majority of immunoreactive mMCP-6 filtered in the column's excluded volume with mMCP-5 and serglycin proteoglycans. These in vitro

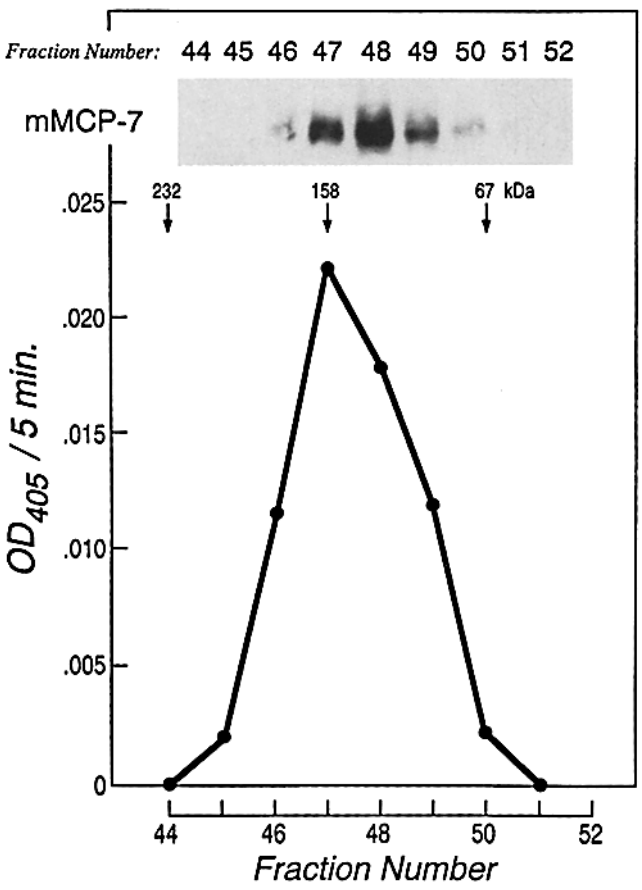

Figure 6. FPLC of mMCP-7 in the plasma of V3 mastocytosis mice. A plasma sample obtained from a FcεRI-activated V3 mastocytosis mouse was applied to a FPLC-Superose column, and a sample of each 0.25-ml fraction was analyzed for tryptase enzymatic activity. The elution profile of three reference proteins, which possess molecular masses of 232, 158, and 67 kD, are depicted. Enzymatic activity was found only in fractions 45–50; fraction 47 contained the maximal amount of enzymatic activity. The proteins in the remainder of each column fraction were precipitated with 10% TCA and assessed by immunoblotting for mMCP-7 (*inset*). Immunoreactive mMCP-7 was found only in fractions 46–50; fraction 48 contained the maximal amount of immunoreactive mMCP-7.

findings again indicate that mMCP-7 differs from mMCP-6 in its ability to dissociate from the macromolecular complex even when exocytosed from an immature cell population of BALB/c mouse mast cells.

Because of the tremendous number of mMCP-6$^+$/mMCP-7$^+$ mast cells in its spleen and liver (41), the V3 mastocytosis mouse represented a more suitable in vivo model system than the normal BALB/c mouse for assessing the fate of exocytosed tryptases beyond the tissue microenvironment of the activated mast cell. In these mice, immunoreactive mMCP-7 was abundant in the plasma 15 and 60 min (Fig. 5) after passive systemic activation. Although mMCP-6 was readily exocytosed from spleen- and liver-localized V3-MC, little or no mMCP-6 was detected in the plasma of the V3 mastocytosis mouse (Fig. 5). Because mMCP-6 did not readily dissociate from the exocytosed granule cores, it is presumed that the large size of the granule core physically hinders the movement of the complex

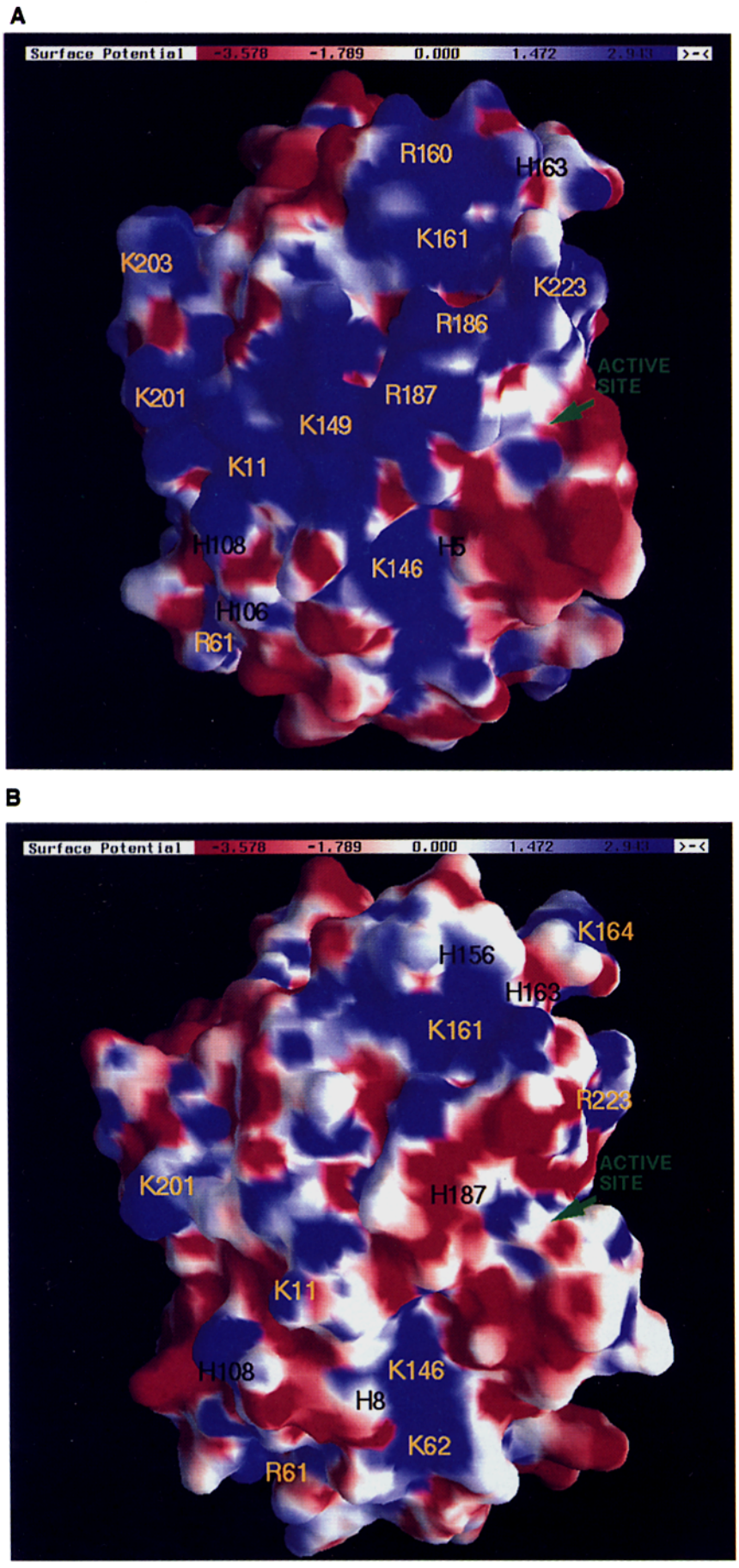

Figure 7. Comparison of the electrostatic properties of the homology models of mMCP-6 (*A*) and mMCP-7 (*B*) at neutral pH. The molecular surfaces of the models are colored by the electrostatic potential, as shown by the color bar on each panel (in units of kT; 1 kT unit = 0.58 kcal/electron mol). (*Yellow*) The positively charged Lys and Arg residues on this face of each tryptase. (*Black*) The His residues. (*Green*) The active site in each protease.

into the blood. A very small amount of immunoreactive mMCP-6 was found in the circulation at the 1- and 4-h time points in only one of five experiments. The failure to reproducibly detect mMCP-6 in plasma could be a consequence of its slower rate of dissociation from the exocytosed granule cores relative to mMCP-7. However, because numerous cell types readily phagocytose exocytosed granule cores (55–58), its tighter association with the granule core might cause mMCP-6 to be catabolized by resident cells in inflammatory sites along with other core-associated proteases.

SDS-PAGE/immunoblot analysis revealed that plasma mMCP-7 is ~32 kD in its monomeric form (Fig. 6), like mBMMC-derived mMCP-7 (42). Whereas plasma mMCP-7 is not covalently bound to a protease inhibitor, the FPLC filtration data indicated that plasma-localized mMCP-7 actually is ~150 kD. The possibility has not been ruled out that plasma mMCP-7 is a monomer that is weakly associated with another protein, but the gel filtration and heparin chromatography findings suggest that this mouse tryptase circulates in the blood predominantly as a tetramer. A preferred tetrameric state for plasma mMCP-7 is compatible with the original description of a human lung mast cell tryptase as a ~140-kD protease consisting of four 31–37-kD monomers (5, 6). Immunoreactive mMCP-7 and tryptase activity exhibited considerable size heterogeneity (Fig. 6). They were detected in the same FPLC fractions, but peak levels of activity and immunoreactive protein differed by one fraction. Human lung mast cell tryptase exhibits maximal activity as a tetramer (31). If mMCP-7 is also optimally active as a tetramer, one explanation for the one fraction difference is partial dissociation of the tetramer.

mMCP-6 and mMCP-7 share 71% sequence identity and have respective net charges of −5 and −10 at neutral pH (2–4). Previous homology modeling and electrostatic potential calculations of mature mMCP-7 and site-directed mutagenesis analysis of recombinant pro-mMCP-7 revealed that mMCP-7 has a His-rich region on its surface (4, 40). This region appears to enable mMCP-7 to interact with serglycin proteoglycans inside the granule at pH 5.5. In extracellular spaces at pH >7.0, His residues are neutral in charge, thereby allowing mMCP-7 to dissociate from serglycin proteoglycan and diffuse away from the exocytosed granule core. The reason for the retention of mMCP-6 in the extracellular matrix may be explained by the apparent electrostatic potential around the tryptase. There is a surface region on mMCP-6 that has 10 positively charged Arg or Lys residues but no Asp or Glu residues (Fig. 7). The region does not cover the active site, although it ends in its vicinity. The region consists of several discontinuous chain segments (e.g., the three-dimensional model predicts that Lys^{11} is adjacent to Lys^{201} and Lys^{149} in mature mMCP-6). This structural feature probably ensures that only properly folded mMCP-6 molecules are stored in the granule bound to serglycin proteoglycan. The positively charged region in mMCP-6 does not overlap with any of the positively charged domains in the mouse mast cell chymases (39) or mMCP-7 (40). Unlike the His-containing proteoglycan-binding region of mMCP-7, the mMCP-6 region remains positively charged at pH >7.0, thereby preventing the dissociation of mMCP-6 from the exocytosed macromolecular complex.

NH_2-terminal amino acid and functional (Fig. 6) analyses indicated that the immunoreactive mMCP-7 in the plasma of the FcεRI-activated V3 mastocytosis mouse is a mature, active enzyme rather than pro-mMCP-7. It is not degraded and is not covalently bound to a protease inhibitor. Although mast cell tryptases purified from the human lung are somewhat resistant to inactivation by plasma-localized protease inhibitors (6, 31), at least one rat mast cell tryptase readily binds the inter-α-trypsin inhibitor (59, 60) and α1-macroglobulin (61) families of protease inhibitors. Such a pathway could exist in BALB/c mice but is overwhelmed by the superimposition of the mastocytosis. However, because mMCP-7 circulates as a multimeric complex rather than as a monomer (Fig. 6), it also could be sterically resistant to inactivation by protease inhibitors. Monomeric mMCP-7 possesses some unique structural features that may hinder its covalent entrapment by protease inhibitors. The lower preponderance of Lys residues on the surface of mMCP-7 (3, 4, 40), coupled with its high degree of glycosylation (42), might prevent the formation of covalent bonds with the reactive γ-Glu residues of α-macroglobulins. In addition, protein-modeling studies (4, 40) revealed that mature mMCP-7 has a surface loop that extends into the active site that could restrict its substrate specificity and also prevent cleavage of the bait regions of various protease inhibitors.

Mouse and human mast cells express at least two tryptases. Based on an ELISA, as much as 88 ng/ml of a human mast cell tryptase has been found in the sera of some patients with mastocytosis and of some patients undergoing systemic anaphylaxis (62, 63). The amount of this immunoreactive protein was insufficient for biochemical characterization, but the finding in the mouse that mMCP-7 selectively dissociates from extracellular-localized granule cores raises the possibility that in other species there is a differential processing of the distinct tryptases in inflammatory sites around activated mast cells. Whereas mMCP-6 is presumed to act locally, perhaps in concert with other complexed secretory granule proteases, enzymatically active mMCP-7 could set up a transient protease gradient in the inflammatory site to allow for proliferation (18, 19) or chemotaxis (64) of other cell types through a mMCP-7–activated receptor, such as those identified for thrombin (65) and trypsin (66).

The technical assistance of Mr. Matthew Webster, Ms. Xuzhen Hu, and Ms. Caroline Coolidge is gratefully acknowledged.

This work was funded by grants AI-23483, AI-22531, AI-31599, AR-07530, AR-36308, HL-48598, and HL-36110 from the National Institutes of Health and a grant from the Hyde and Watson Foundation.

Address correspondence to Dr. N. Ghildyal, Department of Medicine, Harvard Medical School, 250 Longwood Avenue, Room 617, Boston, MA 02115.

Received for publication 7 March 1996 and in revised form 2 May 1996.

References

1. Reynolds, D.S., R.L. Stevens, W.S. Lane, M.H. Carr, K.F. Austen, and W.E. Serafin. 1990. Different mouse mast cell populations express various combinations of at least six distinct mast cell serine proteases. *Proc. Natl. Acad. Sci. USA.* 87: 3230–3234.
2. Reynolds, D.S., D.S. Gurley, K.F. Austen, and W.E. Serafin. 1991. Cloning of the cDNA and gene of mouse mast cell protease-6. Transcription by progenitor mast cells and mast cells of the connective tissue subclass. *J. Biol. Chem.* 266: 3847–3853.
3. McNeil, H.P., D.S. Reynolds, V. Schiller, N. Ghildyal, D.S. Gurley, K.F. Austen, and R.L. Stevens. 1992. Isolation, characterization, and transcription of the gene encoding mouse mast cell protease 7. *Proc. Natl. Acad. Sci. USA.* 89:11174–11178.
4. Johnson, D.A., and G.J. Barton. 1992. Mast cell tryptases: examination of unusual characteristics by multiple sequence alignment and molecular modeling. *Protein Sci.* 1:370–377.
5. Schwartz, L.B., R.A. Lewis, and K.F. Austen. 1981. Tryptase from human pulmonary mast cells: purification and characterization. *J. Biol. Chem.* 256:11939–11943.
6. Smith, T.J., M.W. Hougland, and D.A. Johnson. 1984. Human lung tryptase. Purification and characterization. *J. Biol. Chem.* 259:11046–11051.
7. Miller, J.S., E.H. Westin, and L.B. Schwartz. 1989. Cloning and characterization of complementary DNA for human tryptase. *J. Clin. Invest.* 84:1188–1195.
8. Miller, J.S., G. Moxley, and L.B. Schwartz. 1990. Cloning and characterization of a second complementary DNA for human tryptase. *J. Clin. Invest.* 86:864–870.
9. Vanderslice, P., S.M. Ballinger, E.K. Tam, S.M. Goldstein, C.S. Craik, and G.H. Caughey. 1990. Human mast cell tryptase: multiple cDNAs and genes reveal a multigene serine protease family. *Proc. Natl. Acad. Sci. USA.* 87:3811–3815.
10. Gurish, M.F., J.H. Nadeau, K.R. Johnson, H.P. McNeil, K.M. Grattan, K.F. Austen, and R.L. Stevens. 1993. A closely linked complex of mouse mast cell-specific chymase genes on chromosome 14. *J. Biol. Chem.* 268:11372–11379.
11. Gurish, M.F., K.R. Johnson, M.J. Webster, R.L. Stevens, and J.H. Nadeau. 1994. Location of the mouse mast cell protease 7 gene (*Mcpt7*) to chromosome 17. *Mammal. Genome.* 5: 656–657.
12. Levitt, R.C., and W. Mitzner. 1989. Autosomal recessive inheritance of airway hyperreactivity to 5-hydroxytryptamine. *J. Appl. Physiol.* 67:1125–1132.
13. De Sanctis, G.T., M. Merchant, D.R. Beier, R.D. Dredge, J.K. Grobholz, T.R. Martin, E.S. Lander, and J.M. Drazen. 1995. Quantitative locus analysis of airway hyperresponsiveness in A/J and C57BL/6J mice. *Nature Genetics.* 11:150–154.
14. Hunt, J.E., R.L. Stevens, K.F. Austen, J. Zhang, Z. Xia, and N. Ghildyal. 1996. Natural disruption of the mouse mast cell protease 7 gene in the C57BL/6 mouse. *J. Biol. Chem.* 271: 2851–2855.
15. Clark, J.M., W.M. Abraham, C.E. Fishman, R. Forteza, A. Ahmed, A. Cortes, R.L. Warne, W.R. Moore, and R.D. Tanaka. 1995. Tryptase inhibitors block allergen-induced airway and inflammatory responses in allergic sheep. *Am. J. Respir. Crit. Care Med.* 152:2076–2083.
16. Sekizawa, K., G.H. Caughey, S.C. Lazarus, W.M. Gold, and J.A. Nadel. 1989. Mast cell tryptase causes airway smooth muscle hyperreponsiveness in dogs. *J. Clin. Invest.* 83:175–179.
17. Franconi, G.M., P.D. Graf, S.C. Lazarus, J.A. Nadel, and G.H. Caughey. 1989. Mast cell tryptase and chymase reverse airway smooth muscle relaxation induced by vasoactive intestinal peptide in the ferret. *J. Pharmacol. Exp. Ther.* 248:947–951.
18. Ruoss, S.J., T. Hartmann, and G.H. Caughey. 1991. Mast cell tryptase is a mitogen for cultured fibroblasts. *J. Clin. Invest.* 88:493–499.
19. Cairns, J.A., and A.F. Walls. 1996. Mast cell tryptase is a mitogen for epithelial cells. *J. Immunol.* 156:275–283.
20. Maier, M., J. Spragg, and L.B. Schwartz. 1983. Inactivation of human high molecular weight kininogen by human mast cell tryptase. *J. Immunol.* 130:2352–2356.
21. Caughey, G.H., F. Leidig, N.F. Viro, and J.A. Nadel. 1988. Substance P and vasoactive intestinal peptide degradation by mast cell tryptase and chymase. *J. Pharmacol. Exp. Ther.* 244: 133–137.
22. Gruber, B.L., M.J. Marchese, K. Suzuki, L.B. Schwartz, Y. Okada, H. Nagase, and N.S. Ramamurthy. 1989. Synovial procollagenase activation by human mast cell tryptase. Dependence upon matrix metalloproteinase 3 activation. *J. Clin. Invest.* 84:1657–1662.
23. Stack, M.S., and D.A. Johnson. 1994. Human mast cell tryptase activates single-chain urinary-type plasminogen activator (pro-urokinase). *J. Biol. Chem.* 269:9416–9419.
24. DuBuske, L., K.F. Austen, J. Czop, and R.L. Stevens. 1984. Granule-associated serine neutral proteases of the mouse bone marrow–derived mast cell that degrade fibronectin: their increase after sodium butyrate treatment of the cells. *J. Immunol.* 133:1535–1541.
25. Lohi, J., I. Harvima, and J. Keski-Oja. 1992. Pericellular substrates of human mast cell tryptase: 72,000 dalton gelatinase and fibronectin. *J. Cell. Biochem.* 50:337–349.
26. Schwartz, L.B., T.R. Bradford, B.H. Littman, and B.U. Wintroub. 1985. The fribrinogenolytic activity of purified tryptase from human lung mast cells. *J. Immunol.* 135:2762–2767.
27. Schwartz, L.B., M.S. Kawahara, T.E. Hugli, D. Vik, D.T. Fearon, and K.F. Austen. 1983. Generation of C3a anaphylatoxin from human C3 by mast cell tryptase. *J. Immunol.* 130: 1891–1895.
28. De Young, M.B., E.F. Nemeth, and A. Scarpa. 1987. Measurement of the internal pH of mast cell granules using micro volumetric fluorescence and isotopic techniques. *Arch. Biochem. Biophys.* 254:222–233.
29. Serafin, W.E., H.R. Katz, K.F. Austen, and R.L. Stevens.

1986. Complexes of heparin proteoglycans, chondroitin sulfate E proteoglycans, and [^{3}H]diisopropyl fluorophosphate-binding proteins are exocytosed from activated mouse bone marrow–derived mast cells. *J. Biol. Chem.* 261:15017–15021.
30. Schwartz, L.B., C. Riedel, J.P. Caulfield, S.I. Wasserman, and K.F. Austen. 1981. Cell association of complexes of chymase, heparin proteoglycan, and protein after degranulation by rat mast cells. *J. Immunol.* 126:2071–2078.
31. Schwartz, L.B., and T.R. Bradford. 1986. Regulation of tryptase from human lung mast cells by heparin. Stabilization of the active tetramer. *J. Biol. Chem.* 261:7372–7379.
32. Goldstein, S.M., J. Leong, L.B. Schwartz, and D. Cooke. 1992. Protease composition of exocytosed human skin mast cell protease–proteoglycan complexes. *J. Immunol.* 148:2475–2482.
33. Riley, J.F., and G.B. West. 1955. Tissue mast cells. Studies with a histamine-liberator of low toxicity (compound 48/80). *J. Pathol. Bacteriol.* 69:269–282.
34. Enerbäck, L., and P.M. Lundin. 1974. Ultrastructure of mucosal mast cells in normal and compound 48/80-treated rats. *Cell Tissue Res.* 150:95–105.
35. Levi-Schaffer, F., K.F. Austen, J.P. Caulfield, A. Hein, W.F. Bloes, and R.L. Stevens. 1985. Fibroblasts maintain the phenotype and viability of the rat heparin-containing mast cell in vitro. *J. Immunol.* 135:3454–3462.
36. Alter, S.C., D.D. Metcalfe, T.R. Bradford, and L.B. Schwartz. 1987. Regulation of human mast cell tryptase. Effects of enzyme concentration, ionic strength and the structure and negative charge density of polysaccharides. *Biochem. J.* 248:821–827.
37. Le Trong, H., H. Neurath, and R.G. Woodbury. 1987. Substrate specificity of the chymotrypsin-like protease in secretory granules isolated from rat mast cells. *Proc. Natl. Acad. Sci. USA.* 84:364–367.
38. Saarinen, J., N. Kalkkinen, H.G. Welgus, and P.T. Kovanen. 1994. Activation of human interstitial procollagenase through direct cleavage of the Leu^{83}-Thr^{84} bond by mast cell chymase. *J. Biol. Chem.* 269:18134–18140.
39. Šali, A., R. Matsumoto, H.P. McNeil, M. Karplus, and R.L. Stevens. 1993. Three-dimensional models of four mouse mast cell chymases. Identification of proteoglycan-binding regions and protease-specific antigenic epitopes. *J. Biol. Chem.* 268:9023–9034.
40. Matsumoto, R., A. Šali, N. Ghildyal, M. Karplus, and R.L. Stevens. 1995. Packaging of proteases and proteoglycans in the granules of mast cells and other hematopoietic cells. A cluster of histidines on mouse mast cell protease 7 regulates its binding to heparin serglycin proteoglycans. *J. Biol. Chem.* 270:19524–19531.
41. Gurish, M.F., W.S. Pear, R.L. Stevens, M.L. Scott, K. Sokol, N. Ghildyal, M. Webster, X. Hu, K.F. Austen, D. Baltimore, and D.S. Friend. 1995. Tissue-regulated differentiation and maturation of a v-*abl*–immortalized mast cell–committed progenitor. *Immunity.* 3:175–186.
42. Ghildyal, N., D.S. Friend, R. Freelund, K.F. Austen, H.P. McNeil, V. Schiller, and R.L. Stevens. 1994. Lack of expression of the tryptase mouse mast cell protease 7 in mast cells of the C57BL/6J mouse. *J. Immunol.* 153:2624–2630.
43. Razin, E., J.N. Ihle, D. Seldin, J.-M. Mencia-Huerta, H.R. Katz, P.A. LeBlanc, A. Hein, J.P. Caulfield, K.F. Austen, and R.L. Stevens. 1984. Interleukin 3: a differentiation and growth factor for the mouse mast cell that contains chondroitin sulfate E proteoglycan. *J. Immunol.* 132:1479–1486.
44. Boenisch, T., A.J. Farmilo, and R.H. Stead. 1989. Immunochemical Staining Methods Handbook. S.J. Naish, editor. DAKO Corp., Carpinteria, CA. p. 11.
45. Beckstead, J.H., P.S. Halverson, C.A. Ries, and D.F. Bainton. 1981. Enzyme histochemistry and immunohistochemistry on biopsy specimens of pathologic human bone marrow. *Blood.* 57:1088–1098.
46. Matin, R., E.K. Tam, J.A. Nadel, and G.H. Caughey. 1992. Distribution of chymase-containing mast cells in human bronchi. *J. Histochem. Cytochem.* 40:781–786.
47. Svendsen, L., B. Blombäck, M. Blombäck, and P.I. Olsson. 1972. Synthetic chromogenic substrates for determination of trypsin, thrombin, and thrombin-like enzymes. *Throm. Res.* 1:267–278.
48. Šali, A., and T.L. Blundell. 1993. Comparative protein modeling by satisfaction of spatial restraints. *J. Mol. Biol.* 234: 779–815.
49. Šali, A., and J.P. Overington. 1994. Derivation of rules for comparative protein modeling from a database of protein structure alignments. *Prot. Sci.* 3:1582–1596.
50. Walter, J., W. Steigemann, T.P. Singh, H. Bartunik, W. Bode, and R. Huber. 1982. On the disordered activation domain in trypsinogen. Chemical labeling and low-temperature crystallography. *Acta Crystallogr. Sect. B Struct. Sci.* 38:1462–1472.
51. Laskowski, R.L., M.W. McArthur, D.S. Moss, and J.M. Thornton. 1993. A program to check the stereochemical quality of protein structures. *J. Appl. Cryst.* 26:283–291.
52. Nicholls, A., K.A. Sharp, and B. Honig. 1991. Protein folding and association: insights from the interfacial and thermodynamic properties of hydrocarbons. *Proteins.* 11:281–296.
53. Brooks, B.R., R.E. Bruccoleri, B.D. Olafson, D.J. States, S. Swaminathan, and M.K. Karplus. 1983. CHARMM: a program for macromolecular energy minimization and dynamics calculations. *J. Comp. Chem.* 4:187–217.
54. McNeil, H.P., K.F. Austen, L.L. Somerville, M.F. Gurish, and R.L. Stevens. 1991. Molecular cloning of the mouse mast cell protease-5 gene. A novel secretory granule protease expressed early in the differentiation of serosal mast cells. *J. Biol. Chem.* 266:20316–20322.
55. Smith, D.E., and Y.S. Lewis. 1958. Phagocytosis of granules from disrupted mast cells. *Anat. Rec.* 132:93–111.
56. Welsh, R.A., and J.C. Geer. 1959. Phagocytosis of mast cell granules by the eosinophilic leukocyte in the rat. *Am. J. Pathol.* 35:103–111.
57. Baggiolini, M., U. Horisberger, and U. Martin. 1982. Phagocytosis of mast cell granules by mononuclear phagocytes, neutrophils, and eosinophils during anaphylaxis. *Int. Arch. Allergy Appl. Immunol.* 67:219–226.
58. Rao, P.V.S., M.M. Friedman, F.M. Atkins, and D.D. Metcalfe. 1983. Phagocytosis of mast cell granules by cultured fibroblasts. *J. Immunol.* 130:341–349.
59. Kido, H., Y. Yokogoshi, and N. Katunuma. 1988. Kunitz-type protease inhibitor found in rat mast cells. Purification, properties, and amino acid sequence. *J. Biol. Chem.* 263: 18104–18107.
60. Itoh, H., H. Ide, N. Ishikawa, and Y. Nawa. 1994. Mast cell protease inhibitor, trypstatin, is a fragment of inter-α-trypsin inhibitor light chain. *J. Biol. Chem.* 269:3818–3822.
61. Tsuji, A., T. Akamatsu, H. Nagamune, and Y. Matsuda. 1994. Identification of targeting proteinase for rat α1-macroglobulin in vivo. Mast cell tryptase is a major component of the α1-macroglobulin-proteinase complex endocytosed into

rat liver lysosomes. *Biochem. J.* 298:79–85.
62. Schwartz, L.B., D.D. Metcalfe, J.S. Miller, H. Earl, and T. Sullivan. 1987. Tryptase levels as an indicator of mast cell activation in systemic anaphylaxis and mastocytosis. *N. Engl. J. Med.* 316:1622–1626.
63. Schwartz, L.B., J.W. Yunginger, J. Miller, R. Bokhari, and D. Dull. 1989. Time course of appearance and disappearance of human mast cell tryptase in the circulation after anaphylaxis. *J. Clin. Invest.* 83:1551–1555.
64. Walls, A.F., S. He, L. Teran, M.G. Buckley, K.-S. Jung, S.T. Holgate, J.K. Shute, and J.A. Cairns. 1995. Granulocyte recruitment by human mast cell tryptase. *Int. Arch. Allergy Appl. Immunol.* 107:372–373.
65. Vu, T.-K.H., D.T. Hung, V.I. Wheaton, and S.R. Coughlin. 1991. Molecular cloning of a functional thrombin receptor reveals a novel proteolytic mechanism of receptor activation. *Cell.* 64:1057–1068.
66. Nystedt, S., A.-K. Larsson, H. Åberg, and J. Sundelin. 1995. The mouse proteinase-activated receptor-2 cDNA and gene. Molecular cloning and functional expression. *J. Biol. Chem.* 270:5950–5955.